Available online at

SciVerse ScienceDirect
www.sciencedirect.com

Elsevier Masson France

EM|consulte
www.em-consulte.com/en
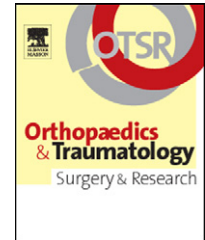
ORIGINAL ARTICLE

Distal locking of femoral nails. Mathematical analysis of the appropriate targeting range

B.K. Moor [a,*], M. Ehlinger [b], Y. Arlettaz [a]

[a] *Orthopaedic and Trauma Department, hôpital du Valais, avenue du Grand-Champsec, 80, 1951 Sion, Switzerland*
[b] *Orthopaedic and Trauma Department, hôpital Hautepierre, 1, avenue Molière, 67098 Strasbourg cedex, France*

Summary
Background: During the last decades, intramedullary nailing has become the standard treatment for diaphyseal fractures of long bones. Numerous innovative techniques and devices have been proposed to simplify distal locking. Each has its own limitations and, as a result, the fluoroscopy-dependent ''free-hand technique'' remains the most popular method. However, radiation exposure to the patient and operating room staff remains a concern.
Methods: Before the development of a new radiation-independent, nail-mounted targeting system, we mathematically analyzed the aiming accuracy that such a system has to achieve. The correctness of this mathematical model was evaluated using a mechanical testing apparatus.
Findings: We found a quite large targeting range for the unimpeded passage of the drill bit through the locking hole of a given nail. Important degrees of nail bending can thereby be compensated. As predicted by the mathematical formula, a 4-mm drill bit passed the distal locking hole of a 320/11 mm femoral nail up to a deflection of ± 13 mm in the coronal plane.
Interpretation: This mathematical model can be considered to be an additional tool for the development of new targeting devices. Combining our mathematical model with data previously published, not only torsional deformation along the longitudinal axis of the nail but also bending in the coronal plane can approximately be neglected. Hence, the three-dimensional aiming process can be simplified to the determination of the interlocking hole of the nail in the sagittal plane provided that the insertion-induced nail deformation *in vivo* stays in the range of that observed *in vitro*.
Level of evidence: Level III. Basic sciences control study.
© 2011 Elsevier Masson SAS. All rights reserved.

* Corresponding author.
E-mail address: bmoor@gmx.ch (B.K. Moor).

Introduction

Accurate aiming of the distal interlocking holes of the nail followed by the insertion of transfixing screws remains a challenging problem in locked intramedullary nailing [1]. Although numerous targeting methods have been proposed, the fluoroscopy-dependent free-hand technique remains the most popular [2—7]. However, radiation exposure to the patient and the staff in the operating room remains a concern. Radiation-independent, conventional proximally mounted targeting devices fail because they do not counter-balance insertion-induced nail deformation [8,9]. To carry out reproducible distal aiming in conjunction with a simple proximally based system, these deforming rotational and bending forces must be respected and compensated by the targeting device.

Our intention in undertaking the present study was to mathematically analyze the range of nail deformation, which is still compatible with successful distal interlocking using a proximally based aiming arm. The accuracy of this mathematical model was evaluated by a mechanical testing apparatus.

Methods

The bending rigidity of an intramedullary nail is dependent upon material properties (elastic modulus) and structural properties (length and area moment of inertia). It is related to the fourth power of the radius of the nail. To simplify matters, the following discussion refers only to the most widely used solid nails and is not conferrable to slotted nails.

Basically, insertion-related bending and rotational forces can deform a nail along its three principal axes: medial—lateral (y), anterior—posterior (z) and rotation along the longitudinal axis (x). These three axes define the following planes: the axial plane (y—z), the sagittal (x—z) and coronal plane (x—y). The distance between the end of the distal nail and the locking holes is given by the geometry of the nail (Fig. 1).

In a cadaver study using a three-dimensional magnetic motion tracking system, Krettek et al. demonstrated that rotational deformation of solid nails is insignificant [8,9]. Insofar, there are deformations only along the y and z axis which have to be considered.

To determine the maximal translation of the nail in the coronal plane (x—y), which still allows contactless progress of the drill bite through the distal nail hole, the following equation was assumed. To simplify matters, we consider no deflection in the sagittal plane. J2 represents the distance from the drill bit to the margin of the nearby interlocking hole of the nail, and J1 the distance to the distant one (Fig. 2). Alpha (α) represents the deflection angle of the nail in the coronal plane. It is defined as $0° < \alpha < 90°$; R is the length of the nail and D_N its diameter. D_H stands for the diameter of the interlocking hole of the nail, and D_D the diameter of the drill bit.

$$J1 = \left(R + \frac{1}{2}D_H\right)\cos\alpha - \frac{1}{2}D_N\sin\alpha - \left(R - \frac{1}{2}D_D\right)$$
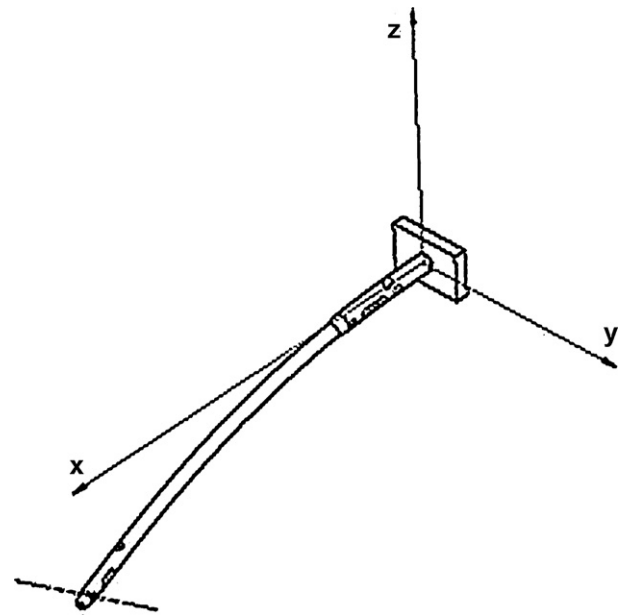
Figure 1 Rectangular coordinate system to define the three principal axes along which an intramedullary nail can be deformed during implantation: medial—lateral (y), anterior—posterior (z) and rotation along the longitudinal axis (x).
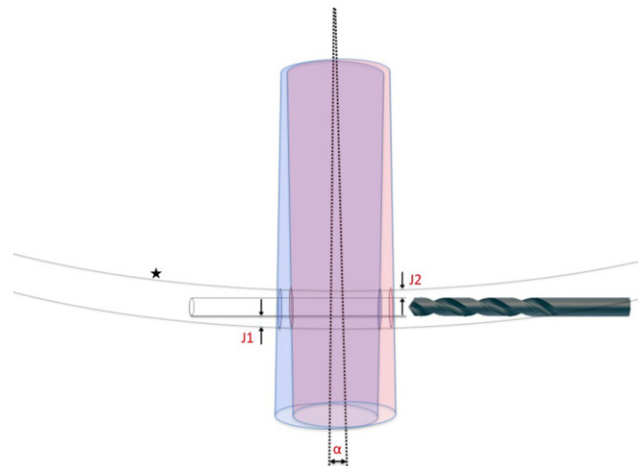
Figure 2 Passage of a drill bit through the distal locking hole of a nail (schematic). J2 represents the distance from the drill bit to the margin of the nearby interlocking hole of the nail. J1 is the distance to the distant one. Alpha (α) represents the deflection angle of the nail in the coronal plane. Contactless drilling is only possible provided that J1 as well as J2 are greater or equal to 0.

$$J2 = \left(R + \frac{1}{2}D_D\right) - \left(\left(R - \frac{1}{2}D_H\right)\cos\alpha + \frac{1}{2}D_N\sin\alpha\right)$$

Contactless drilling is only possible provided that J1 as well as J2 are greater or equal to 0. Analogous considerations can be applied for translation in the sagittal (x—z) plane.

To evaluate the accuracy of our mathematical model, a mechanical testing apparatus was developed (Fig. 3). The device consisted of a bench in which a solid, commercially

Figure 3 Overview of the testing apparatus. An intramedullary nail (1) with a proximally mounted aiming arm (2) was solidly fixed on a bench (3). After calibration of the system, the nail was progressively bended by dressing the clamp (arrow) until the passage of the drill bit (4) through the locking hole of the nail was not possible. The amount of nail bending was indicated on the calliper (5).

Figure 4 Calibration of the testing apparatus in the neutral position without external forces being applied to the nail.

available intramedullary nail (Sirus intramedullary nail, Zimmer, Warsaw, IN, USA) with variable diameter and length was firmly anchored. The proximal end of the nail was connected to a targeting arm, whereas the distal end was linked to a calliper. After determination of the zero position (Fig. 4), the nail was progressively bent in the coronal (x—y) plane in steps of 0.5 mm, until drill—nail contact occurred during the passage of the drill bit through the interlocking hole of the nail.

Results

As an example, we consider a case with a solid standard nail of diameter 11 mm, of length 320 mm, with a diameter of the interlocking hole of 5 mm and the use of a drill bit of diameter 4 mm.

According to the above-mentioned equation, a contactless passage of the drill bit can be guaranteed up to a nail deflexion of ± 13 mm, corresponding to a targeting range of

Table 1 Predictive mathematical results with a nail length of 320 mm and a diameter of 11 mm.

Nail bending $\triangle y$ (mm)	Distance ''j1'' (mm)	Distance ''j2'' (mm)
0.00	0.5000	0.5000
1.00	0.4812	0.4844
2.00	0.4593	0.4718
3.00	0.4343	0.4624
4.00	0.4061	0.4561
5.00	0.3747	0.4528
6.00	0.3402	0.4527
7.00	0.3025	0.4557
8.00	0.2617	0.4617
9.00	0.2177	0.4709
10.00	0.1706	0.4832
11.00	0.1203	0.4986
12.00	0.0669	0.5171
13.00	0.0103	0.5387
13.50	−0.0191	0.5506
14.00	−0.0494	0.5634

Table 2 Targeting range depending upon the length and diameter of the nail.

Nail diameter (mm)	Length 320 mm	Length 480 mm
9	13.5	17.5
10	13.5	17
11	13	17
12	12.5	16.5
13	12	16
14	12	15.5

26 mm in the coronal and sagittal plane (Table 1). Applying these considerations to standard femoral nails with increasing lengths from 320 mm to 480 mm, using the same diameter of the distal targeting hole of the nail and the same drill bit, the targeting range varies as follows: for a nail diameter of 10 mm from 27 to 34 mm, for a nail diameter of 11 mm from 26 to 34 mm, and for a nail diameter of 12 mm from 25 to 33 mm (Table 2). Equivalent calculations can be made for different diameters of the targeting hole of the nail as well as various diameters of the drill bit.

Our mathematical analyses were verified on the testing frame. The results of this experimental part were in accordance with the mathematical prediction. As calculated in Table 1, contactless passage of a 4-mm drill through the distal interlocking hole of a 320/11 mm femoral nail was limited to a maximal nail-bending of 13 mm. Due to the elasticity of the system and especially of the drill bit, the latter could even pass the interlocking hole of the nail up to a nail deformation of 15.5 mm (Fig. 5). However, this was accompanied with severe drill—nail contact.

Discussion

The indication of intramedullary nailing for the treatment of fractures of the femoral shaft has been greatly expanded by the technique of distal interlocking [10—15].
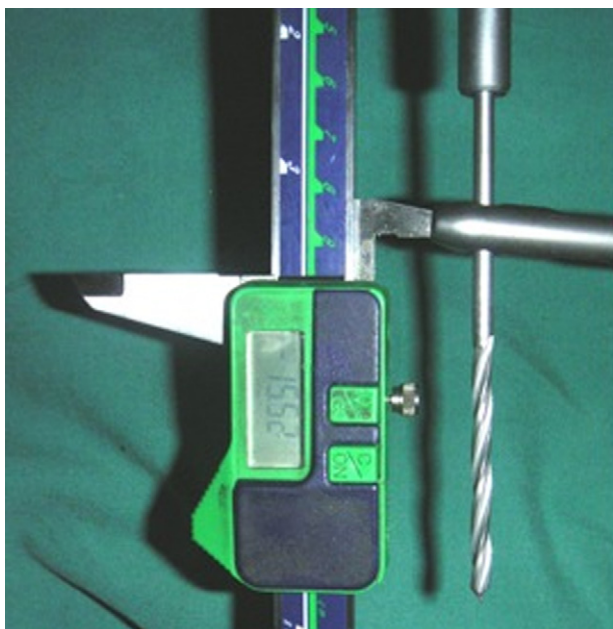
Figure 5 Due to the interplay of the system, the drill bit could pass up to a nail deformation of 15.5 mm. However, this was accompanied by severe drill—nail contact with slight bending of the drill bit.

However, radiation exposure to the patient and operating room staff remains a concern. In a prospective study of 65 orthopaedic procedures undertaken with fluoroscopic assistance, Sanders et al. showed that intramedullary nailing involved significantly more fluoroscopic time than did other types of procedure [16]. The greatest level of radiation was recorded during intramedullary femoral nailing that involved distal interlocking. In an attempt to reduce this potentially harmful radiation burden, several authors proposed fluoroscopy-independent, proximally mounted targeting systems [17,18]. Unfortunately, most of them failed because these simple aiming arms do not compensate for insertion-induced nail deformation [8,9].

Before the development of a new radiation-independent, nail-mounted targeting device, we mathematically analyzed the aiming accuracy that such a system has to achieve. Our mathematical model revealed a quite large targeting range for the passage of the drill bit through the locking hole of a given nail, which allows compensation of even an important degree of nail bending. As predicted, contactless passage of a 4-mm drill through the distal interlocking hole of a 320/11 mm femoral nail was feasible up to a nail deflexion of ±13 mm in the coronal plane. If drill—nail contact is accepted, successful drilling is possible even up to a nail deformation of 15.5 mm due to the elasticity of the system. However, this could lead to a deformation of the locking screw, and may be a potential source for future failure of the hardware.

If we choose a short nail (little R), without changing the other values, J1 and J2 will be less than for a long nail. This indicates a smaller targeting range for a short nail than for a long nail and *vice versa*. Conversely, a short nail is stiffer than a long nail and thus there will be less nail deformation that has to be overcome. If the diameter of the interlocking

hole of the nail increases, J1 and J2 increase accordingly. This means a lager targeting range for a bigger interlocking hole. Otherwise, J1 and J2 decrease with lager diameters of the nail and the drill bit. However, as already mentioned for the length of the nail, an increasing diameter of the nail is accompanied by growing bending rigidity, and thus the smaller targeting range may be still sufficient to allow successful interlocking.

In an experimental study on 20 intact human cadaveric tibiae, Krettek et al. demonstrated an average implant deformation in the sagittal plane of -7.8 ± 5.8 mm (range, 19.2 mm) and in the coronal plane of -4.5 ± 3.5 mm (range, 14.3 mm) for combined 8-mm and 9-mm nail diameters, respectively [8]. In a similar study on 20 intact fresh human cadaveric femora, the average deformation of a 9-mm solid nail averaged -3.1 ± 4.3 mm (range, 15.2 mm) and 18.2 ± 10.0 mm (range, 47.8 mm) in the sagittal plane and coronal plane, respectively [9]. Rotational deformation along the longitudinal axis of the nail was insignificant in both studies. Combining these data with the results of the present study indicates that, for distal tibial locking, the accuracy of a simple proximally mounted targeting device should be almost sufficient, whereas for femoral locking an adjustment (at least in one plane) seems to be essential. However, these are data of *in vitro* experiments using intact cadaveric bones. Up until now, the amount of nail deformation in *in vivo* conditions and in the context of a fracture is unknown. Furthermore our model is a simplification of the 3D nature of the nail deformation. If there is a combined nail translation in the coronal and sagittal plane, already minor deformities will lead to failure of the locking process. However, our data suggest that a perfect adjustment of a proximally mounted aiming arm in one plane is sufficient. For instance in tibial nailing, an additional targeting device, that allows perfect alignment in the sagittal plane would be sufficient as the deformation in the coronal plane is negligible.

Conclusion

The mathematical model described in this contribution can be considered to be an additional tool for the development of new targeting devices. As previously demonstrated, insertion-induced rotational deformation in intramedullary nailing is insignificant [8,9]. Moreover, our formula predicts a large targeting range in the sagittal and coronal plane. Combining our mathematical model with the data of Krettek et al., not only torsional deformation along the longitudinal axis of the nail but also bending in the coronal plane can approximately be neglected. Hence, the three-dimensional aiming process can be simplified to the determination of the interlocking hole of the nail in the sagittal plane provided that the insertion-induced nail deformation *in vivo* stays in the range of the deformation observed *in vitro*.

Disclosure of interest

The authors declare that they have no conflicts of interest concerning this article.

Acknowledgements

References

[1] Winquist RA. Locked femoral nailing. J Am Acad Orthop Surg 1993;1—2:95—105.

[2] Kelley SS, Bonar S, Hussamy OD, Morrison JA. A simple technique for insertion of distal screws into interlocking nails. J Orthop Trauma 1995;9—3:227—30.

[3] Hashemi-Nejad A, Garlick N, Goddard NJ. A simple jig to ease the insertion of distal screws in intramedullary locking nails. Injury 1994;25—6:407—8.

[4] Hudson I. Locking nailing: an aid to distal targetting. Injury 1989;20—3:129—30.

[5] MacMillan M, Gross RH. A simplified technique of distal femoral screw insertion for the Grosse-Kempf interlocking nail. Clin Orthop Relat Res 1988;226:252—9.

[6] Rao JP, Allegra MP, Benevenia J, Dauhajre TA. Distal screw targeting of interlocking nails. Clin Orthop Relat Res 1989;238:245—8.

[7] Riley SA. Radiation exposure from fluoroscopy during orthopedic surgical procedures. Clin Orthop Relat Res 1989;248:257—60.

[8] Krettek C, Mannss J, Konemann B, Miclau T, Schandelmaier P, Tscherne H. The deformation of small diameter solid tibial nails with unreamed intramedullary insertion. J Biomech 1997;30—4:391—4.

[9] Krettek C, Mannss J, Miclau T, Schandelmaier P, Linnemann I, Tscherne H. Deformation of femoral nails with intramedullary insertion. J Orthop Res 1998;16—5:572—5.

[10] Johnson KD, Greenberg M. Comminuted femoral shaft fractures. Orthop Clin North Am 1987;18—1:133—47.

[11] Johnson KD. Internal fixation of distal femoral fractures. Instr Course Lect 1987;36:437—48.

[12] Zuckerman JD, Veith RG, Johnson KD, Bach AW, Hansen ST, Solvik S. Treatment of unstable femoral shaft fractures with closed interlocking intramedullary nailing. J Orthop Trauma 1987;1—3:209—318.

[13] Kempf I, Grosse A, Beck G. Closed locked intramedullary nailing. Its application to comminuted fractures of the femur. J Bone Joint Surg Am 1985;67—5:709—20.

[14] Thoresen BO, Alho A, Ekeland A, Stromsoe K, Folleras G, Haukebo A. Interlocking intramedullary nailing in femoral shaft fractures. A report of forty-eight cases. J Bone Joint Surg Am 1985;67—9:1313—20.

[15] Winquist RA, Hansen Jr ST, Clawson DK. Closed intramedullary nailing of femoral fractures. A report of five hundred and twenty cases. J Bone Joint Surg Am 1984;66—4:529—39.

[16] Sanders R, Koval KJ, DiPasquale T, Schmelling G, Stenzler S, Ross E. Exposure of the orthopaedic surgeon to radiation. J Bone Joint Surg Am 1993;75—3:326—30.

[17] Soyka P, Bussard C. Interlocking intramedullary nailing. A solid aiming device for distal locking. Helv Chir Acta 1990;57—1:117—20.

[18] Berentey G. Neues Zielgerät für die distale Verriegelungsnagelung. Hefte Unfallheilkd 1983;165:260—2.